Quaternary Science Advances 19 (2025) 100292

Contents lists available at ScienceDirect

Quaternary Science Advances

journal homepage: www.sciencedirect.com/journal/quaternary-science-advances

Review

Converging evidence constrains late pleistocene bering land bridge history

Ciara Wanket [a,*], Samuel Kodama [b], Jonas Oppenheimer [c], Scott Cocker [d], Emma Steigerwald [a], Duane Froese [d], Beth Shapiro [a], Tamara Pico [b], Jesse Farmer [e]

[a] Department of Ecology and Evolutionary Biology, University of California, Santa Cruz, Santa Cruz, CA, USA
[b] Department of Earth and Planetary Sciences, University of California, Santa Cruz, Santa Cruz, CA, USA
[c] Department of Biomolecular Engineering, University of California, Santa Cruz, Santa Cruz, CA, USA
[d] Department of Earth and Atmospheric Sciences, University of Alberta, Edmonton, Alberta, Canada
[e] School of the Environment, University of Massachusetts Boston, Boston, MA, USA

ARTICLE INFO

Keywords:
Bering land bridge
Paleogenomics
Paleoceanography

ABSTRACT

The Bering Land Bridge was an important biotic corridor and climatic modifier during the Pleistocene (2.58 million to 11,700 thousand years ago [ka]). Understanding when the land bridge was most recently exposed reveals insights into past climate, the modern distribution of plants and animals, and potential human migration into the Americas. While the timing of the most recent flooding of the land bridge has been constrained to during the last deglaciation, the timing of its most recent exposure before the Last Glacial Maximum (LGM, 26.5–19 ka) is less clear. Here, we combine data from three disciplines— paleoceanography, sea level reconstruction, and terrestrial paleogenomics—to constrain the most recent exposure of the Bering Land Bridge to shortly before the LGM, 30–40 kyr later than previously suggested by comparisons of eustatic sea level reconstructions with the modern Bering Strait Sill depth. These results have implications for understanding the timing and nature of human arrival in the Americas and highlight the importance of interdisciplinary collaboration across paleoclimatology and paleoecology for refining Pleistocene environmental history.

1. Significance statement

The timing of Bering Land Bridge exposure has important implications for past climate and species migrations– including for when and how humans entered the Americas from Asia. By combining paleoceanography, sea level reconstructions, and ancient DNA evidence, we show that the most recent exposure of the land bridge occurred 40–35,000 years ago. This timing, significantly later than previously thought and within 15,000 years of the peak of the last ice age, suggests that humans inhabited the land bridge region soon after it was exposed. Our interdisciplinary findings emphasize the power of collaboration for addressing longstanding scientific problems that stretch across research domains.

2. Introduction and background

During the Pleistocene, climate alternated between cold glacial periods and warmer interglacial periods, driving the growth and decay of continental ice sheets and consequent rise and fall of global sea level (Berends et al., 2021). Following the opening of the Bering Strait in the latest Miocene (Hall et al., 2023), its shallow water depth (only 53 m at its deepest point today) made the region prone to intermittent subaerial exposure by lowered global sea level during glacial periods. When flooded, the Bering Strait provides the only Northern Hemisphere link between the Pacific and Atlantic Oceans (Fig. 1a). At times of exposure, the Bering Land Bridge (BLB) connected North America with Eurasia to create the region known as Beringia, which stretched from Russia's Lena River in the west to Yukon's Mackenzie River in the east (Fig. 1b).

While it has been established that the BLB was fully flooded by 11 ka (Dyke et al., 1996; England and Furze, 2008; Jakobsson et al., 2017; Pico et al., 2020), the timing of BLB exposure before global sea-level reached its lowest point (lowstand) during the Last Glacial Maximum (26.5–19 ka; Clark et al., 2009) is less certain. Direct evidence on BLB formation is lacking, as there are few sedimentary cores across the Beringia shelf, and none on the Bering Strait itself (Mann and Gaglioti, 2024). Furthermore, when sea level rose and flooded the BLB during the last deglaciation, earlier sedimentary deposits may have been eroded by wave action and/or currents (e.g., Elias et al., 1996).

* Corresponding author. CBB/EE Biology Ecology and Evolutionary Biology, UCSC/Coastal Biology Building, 130 McAllister Way, Santa Cruz, CA 95060, USA.
E-mail address: cwanket@ucsc.edu (C. Wanket).

https://doi.org/10.1016/j.qsa.2025.100292
Received 21 March 2025; Received in revised form 7 August 2025; Accepted 10 August 2025
Available online 12 August 2025

Given the sparsity of direct local constraints, Bering Strait sea level has generally been assumed to match global mean sea level. On the basis of earlier global sea level reconstructions, most studies have assumed the BLB most recently formed near 70 ka during a sea-level fall associated with the transition from interglacial Marine Isotope Stage (MIS) 5a to glacial MIS 4 (Hu et al., 2012; Mann and Gaglioti, 2024). In this case, the BLB existed for ~45 kyr before the LGM (Mann and Gaglioti, 2024). However, addressing BLB exposure through global sea-level reconstructions is challenged by uncertainties in global ice volume, with recent studies arguing for high globally averaged sea level in the period before the LGM (de Gelder et al., 2022). Furthermore, local relative sea level in Beringia can vary substantially from the global average, due to effects from near-field ice sheet growth and retreat (e.g., Farmer et al., 2023; Hu et al., 2010; Pico et al., 2020). A recent study tracked the inflow of Pacific waters into the Arctic and found that the BLB formed at ~36 ka, only ~10 kyr before the LGM, and dramatically later than earlier studies assumed (Farmer et al., 2023). Constraining the timing of this most recent BLB exposure is important for understanding global ocean circulation patterns, the paleoclimate of Beringia, and migration between Eurasia and the Americas– including the paleoenvironment humans would have experienced as they migrated from Asia into North America.

The timing of BLB exposure offers a key test for hypotheses about the drivers of climate and sea level fluctuations during the last glacial period. The Bering Strait is a conduit for relatively fresher Pacific waters to flow into the saltier Arctic Ocean. The freshening of Arctic surface waters makes them less dense and, in turn, weakens the Atlantic Meridional Overturning Circulation, affecting global climate (Brierley and Fedorov, 2016; Hu et al., 2012). One hypothesis is that the abrupt climate fluctuations during the last glacial period were only possible with an exposed BLB (De Boer and Nof, 2004; Hu et al., 2010). Accurately defining intervals of BLB exposure is a necessary test for this hypothesis.

Understanding the status of the land bridge over the last 50 kyr would additionally help to address significant unresolved questions about the Beringian paleoclimate. Whether the Bering Strait was flooded was a critical factor in Beringian climate during the late Pleistocene. When flooded, the Bering Strait drove cooler summers and warmer winters, a pattern evident in eastern Beringia during early Holocene post-glacial warming (Bartlein et al., 2015). In contrast, the exposed land bridge increased continentality, reducing the moderating influence of coastal climates and causing extreme summer and winter temperatures in interior regions (Daniels et al., 2021). However, the habitat of the exposed land bridge remains a topic of active debate, with some controversy over whether the bridge was a moderately wet (mesic) region within the otherwise arid mammoth-steppe biome that dominated the unglaciated regions of northern hemisphere (Elias et al., 1996; Elias and Crocker, 2008; Guthrie, 2001), or rather a continuation of the arid mammoth-steppe with some fine-scale regional heterogeneity (Ager and Phillips, 2008; Goetcheus and Birks, 2001).

Timing the BLB exposure is paramount for understanding the evolution and dispersal of many plant and animal species. When flooded, the Bering Strait facilitated the migration of marine species such as mollusks (England and Furze, 2008; Hall et al., 2023), planktonic pteropods (Abyzova et al., 2025), and gray whales (Alter et al., 2007) between the Pacific and Arctic Oceans. When exposed, the BLB was a biogeographically pivotal region, facilitating major biotic interchange between Eurasia and the Americas and enabling the establishment of species such as horses (Vershinina et al., 2021) and camels (Heintzman et al., 2015) in Eurasia, and wolves (Loog et al., 2020) and bison (Froese et al., 2017) in North America. Additionally, the timing and route of human dispersal into the Americas are thought to be tied to the timing of BLB exposure (Hoffecker et al., 2014; Praetorius et al., 2023; Wooller et al., 2018) and are of particular interest to anthropologists and paleoclimatologists seeking to reconstruct the environmental context of early human migration pathways.

An interdisciplinary approach that integrates multiple, independent perspectives on the history of the BLB can remedy field-specific challenges in dating the most recent BLB exposure event. Here, we expand on previous work by Farmer et al. (2023) to synthesize findings from three distinct approaches– paleoceanographic isotopic records, paleo-sea level reconstructions, and megafaunal population genetics– covering BLB history over the last 50 kyr (Fig. 2). To foster interdisciplinary collaboration and understanding, we provide general background information and perspectives on the future directions of each approach. Together, these observations support the idea that the BLB was last exposed shortly before the LGM, over 30 kyr later than traditionally assumed (Hu et al., 2012; Mann and Gaglioti, 2024).

3. Paleoceanography

3.1. Background

A remarkable oceanographic feature of the Bering Strait is its steady northward flow. Long observed by local Indigenous communities (e.g., Raymond-Yakoubian et al., 2014), northward flow across the Bering Strait was first documented in European science traditions by Vitus Bering's 1728 expedition (Coachman and Aagaard, 1966). Given the shallow depth of the Bering Strait, flow through the strait would be expected to be wind-driven. However, long-term observations show that northward transport persists over monthly, annual and interannual timescales, independent of seasonal wind patterns (Woodgate, 2018). Instead, this northward transport is thought to arise from warmer, fresher Bering Sea waters raising its sea level relative to the Arctic Ocean. The resulting sea level height difference creates a pressure head, which pushes Bering Sea waters northward into the Arctic Ocean (Woodgate, 2018 and references therein) and forms the fundamental basis for employing Arctic Ocean sediments for reconstructing Being Strait presence/absence and flow strength in the geological past.

The total northward transport through the Bering Strait is on the order of 1 Sverdrup (1,000,000 cubic meters per second; Coachman and Aagaard, 1966; Woodgate, 2018 and references therein). Although this is small compared to the global ocean overturning circulation, the Bering Strait's transport is notable for its profound effects on the structure and properties of the "downstream" Arctic Ocean (Fig. 3). The Bering Strait inflow accounts for approximately one third of the Arctic Ocean's total freshwater input (Aagaard and Carmack, 1989; Serreze et al., 2006), and about 20 %, 35 %, and 60 % of its total inputs of the nutrients nitrate, phosphate, and silicate, respectively (Torres-Valdés et al., 2013). Notably, these inputs end up concentrated near the surface ocean rather than diffused throughout the water column (Fig. 3). Ocean waters are classified into water masses based on density; at the near-freezing temperatures of the Arctic Ocean, density is set largely by salinity. The relatively fresh Bering Strait inflow waters are less salty than Atlantic waters inflowing from the Barents Sea and Fram Strait. Accordingly, these Pacific-sourced waters end up as a distinct "upper halocline" water mass within the Arctic Ocean. Here they act as a nutrient reservoir to the euphotic zone and thereby help set the properties of biological materials growing in the Arctic Ocean surface.

Pacific-sourced waters in the Arctic Ocean are readily traced by their unique composition. In addition to their low salinity and elevated nutrient concentrations, Pacific-sourced waters carry distinct nitrate to phosphate ratios (Jones et al., 1998; Newton et al., 2013), nitrate to dissolved oxygen ratios (Alkire et al., 2019), trace element concentrations (e.g., gallium; Whitmore et al., 2020), stable isotope ratios of nitrate (Farmer et al., 2021; Fripiat et al., 2018; Granger et al., 2018) and trace elements (e.g., Nd; Porcelli et al., 2009; Song et al., 2022), as well as unique clay mineral assemblages (e.g., Naidu et al., 1982). Studies of past Pacific-Arctic connection through the Bering Strait are premised on these unique features of Pacific water inflow being preserved within Arctic Ocean seafloor sediments (Fig. 3).

3.2. Arctic sediment records of Bering Strait inflow

With sedimentary tools available to distinguish Pacific-sourced waters in the Arctic Ocean, the next question is where such tools could most fruitfully be applied. From a sedimentation perspective, the Arctic is effectively two depositional zones: a shallow continental shelf and a deep basin (e.g., Bluhm et al., 2015). On the extensive continental shelves, such as in the Chukchi Sea north of the Bering Strait, seafloor sediments accumulate rapidly from high rates of primary productivity and terrigenous input. When recovered in stratigraphic order through sediment sampling, the resulting sediments can allow for centennial-scale resolution of Bering Strait inflow. However, this resolution comes at the expense of longevity: Shelf sedimentation has only occurred since the shelves were flooded by postglacial sea-level rise, which created accommodation space for sediment deposition (since roughly 10 ka). Thus, shelf sediment reconstructions of Bering Strait inflow are currently only feasible for the Holocene (Song et al., 2022).

In contrast, the deep Arctic basins (Canada, Makarov, Amundsen and Nansen) maintained accommodation space throughout the Quaternary sea level lowstands. Unfortunately, these basins tend to be sediment-limited: Holocene sedimentation rates average at most 2 cm per 1000 years due to low primary productivity and inefficient transport of terrigenous sediments by sea ice (Polyak et al., 2009). Moreover, Holocene sedimentation appears to be a geological best-case scenario for the last 50 kyr: Sedimentation rates during the LGM appear to have been reduced by an order of magnitude, or sedimentation may have even stopped completely in some locations during the LGM (Polyak et al., 2009). Thus, while sedimentary records in the Arctic basins allow for longer-term reconstructions of Bering Strait inflow, they are at best millennial-scale resolution and are prone to hiatuses when sediment deposition was greatly reduced (for instance in cold climates like the LGM).

Existing reconstructions of Bering Strait inflow from Arctic sediment cores largely fall within these two depositional regimes. Clay mineral and Nd isotope reconstructions from the Chukchi Sea shelf have been interpreted to indicate maximum of Bering Strait inflow during the mid-Holocene ca. 6 ka, although the estimated timing and duration of this inflow maximum varies between locations (e.g., Song et al., 2022; Stein et al., 2017; Yamamoto et al., 2017). Foraminifera-bound N isotopes from the Canada Basin trace the history of Bering Strait flooding and exposure back to 50 ka by tracking the unique isotopic composition of nitrate sourced from the Bering Strait inflow (Fig. 2a). These records indicate that the Bering Strait was flooded prior to the LGM up until ~36 ka (Farmer et al., 2021, 2023).

4. Sea level reconstructions

4.1. Background

Ice volume variations throughout the last glacial cycle are a direct and sensitive measure of ice-age climate change and provide a means of investigating how ice sheets respond to dynamic climate conditions. However, the magnitude and timescale of global ice sheet fluctuations during the last ice age prior to the LGM are highly uncertain (Batchelor et al., 2019; Dalton et al., 2022; Gowan et al., 2021; Pico, 2022; Pico et al., 2017).

Histories of ice sheet volume can be estimated by mapping ice sheet extent via terminal moraines (sediment deposits that accumulate around the periphery of an ice sheet) or cosmogenic exposure dating, which indicates when a surface previously covered by ice became exposed (Fig. 4; Stokes et al., 2015). Ice sheet volume can then be reconstructed by pairing records of ice sheet extent with measurements of past ice sheet thickness via methods such as cosmogenic age-elevation transects (Stone et al., 2003), or modeling equilibrium ice thickness profiles for a given ice sheet extent, assuming specific basal conditions (i.e., topography and basal shear stress; Fig. 4; Gowan et al., 2021). However, measuring ice sheet thickness via cosmogenic age-elevation transects is restricted to areas of high relief and the erosive nature of an ice sheet often limits the geologic record to record the most recent ice sheet advance, leaving sparse geologic constraints of any kind before the LGM (Dalton et al., 2022; Stokes et al., 2015).

Changes in global ice sheet volume have been estimated using benthic (bottom water) and planktic (surface water) foraminifera. Oxygen isotope records ($\delta^{18}O$) of benthic foraminifera from deep-sea sediments can be used to estimate global ice sheet volume due to the isotopic enrichment of ^{18}O in sea water as growing terrestrial ice sheets trap lighter ^{18}O (Spratt and Lisiecki, 2016; Waelbroeck et al., 2002). Planktic foraminifera from marginal seas where exchange with the open ocean is restricted, such as the Red Sea and Mediterranean Sea, can also record global ice sheet volume (Grant et al., 2014; Rohling et al., 2014; Siddall et al., 2003). However, the accuracy of ice volume inferences based on oxygen isotope records is limited by regional variability, uncertainties in the conversion from $\delta^{18}O$ related to temperature, and the mean $\delta^{18}O$ of continental ice (Siddall et al., 2004; Waelbroeck et al., 2002).

A more direct proxy for global ice sheet variations are geologic sea level records. Sea level can be recorded through a diverse range of geologic markers, including marine terraces, beach deposits, sedimentary and biological facies, and coral reefs (Hanebuth et al., 2006; Lambeck and Chappell, 2001; Muhs et al., 2012; Yokoyama et al., 2000). However, geological markers of relative sea level are spatially and temporally sparse, and before they can provide estimates of global ice sheet volume, they must be corrected for a variety of contaminating signals such as tectonics, dynamic topography, and, most notably, glacial isostatic adjustment (de Gelder et al., 2022; Hibbert et al., 2016; Lambeck et al., 2014; Moucha et al., 2008).

Glacial isostatic adjustment (GIA) is the gravitational, rotational, and solid-Earth response to the growth and decay of ice sheets over glacial cycles. The redistribution of surface mass loads over glacial cycles perturbs the Earth's gravitational field through crustal deformation and direct self-attraction, in addition to shifting the Earth's rotation axis. The redistribution of water is, in turn, governed by this gravitational perturbation since the sea surface must remain as an equipotential in a static sea-level theory (Farrell and Clark, 1976). Therefore, ice sheet growth and melt produce a complex spatio-temporal pattern of sea level change that is dependent on the full history of the surface mass (ice and ocean water) load (Fig. 4). Thus, geological sea-level markers record sea level at their specific location (i.e., relative sea level) and need to be corrected for glacial isostatic adjustment in order to provide information on past global sea level and global ice volume (e.g., Lambeck et al., 2014).

Nevertheless, even when sea-level markers can be corrected for contaminating signals, the record of sea-level markers during times when global ice sheet volume was larger than present are sparse because most sea-level markers that record lower global sea level are presently submerged. Accessible sea-level markers that record sea level lowstands are limited to locations that are tectonically uplifted (de Gelder et al., 2022; Malatesta et al., 2021; Peltier and Fairbanks, 2006).

Constraints on ice volumes prior to the LGM provide an illustrative case of the uncertainty characterizing global sea-level change across the last glaciation phase (from ~110 to 26 ka; Pico, 2022). For example, over the time period from 45 to 35 ka, disagreement between estimates of ice-equivalent sea level span as much as ~60 m, ranging from −100 to −38 m according to records based on oxygen isotopes (Peltier and Fairbanks, 2006; Waelbroeck et al., 2002) and GIA-analysis of sea-level markers (Gowan et al., 2021; Pico et al., 2016, 2017). Global mean sea level during the sea level lowstand at the LGM has been established at −130 m (Austermann et al., 2013; Yokoyama et al., 2000). Therefore, within current disagreement, in the 15 kyr period leading up to the LGM, global ice volume may have increased by more than a factor of 3 (by ~92 m sea-level equivalent; Pico et al., 2017) or by less than one-half (by ~30 m sea level equivalent; Peltier and Fairbanks, 2006).

4.2. Relative sea level history of the Bering Strait

The shallow Bering Strait (53 m depth; Fig. 1) acts as a unique, intermediate relative sea-level bound, as global mean sea level during the last glaciation phase oscillated between a range of −10 and −100 m (Pico, 2022; Siddall et al., 2008), exposing and submerging the strait whenever relative sea level rose or fell above the sill depth. The depth of the Bering Strait sill likely varied through time due to sedimentation, erosion, thermokarst inflation or deflation, and crustal uplift or subsidence due to local tectonics or dynamic topography (Mann and Gaglioti, 2024). Indeed, there is evidence for long-term uplift from high elevation sea-level markers dated to the Pliocene (Kaufman and Brigham-Grette, 1993). While these processes are poorly constrained, there has likely been <10 m of vertical elevation change at the Bering Strait since 40 ka (Mann and Gaglioti, 2024). Furthermore, improved bathymetric reconstructions will resolve the Bering Strait sill depth with greater accuracy (Danielson et al., 2015).

Determining relative sea level at the Bering Strait can potentially distinguish between different proposed ice sheet histories, which predict contrasting scenarios for when the BLB was exposed. For example, we plotted relative sea level at the Bering Strait corrected for glacial isostatic adjustment based on ice histories defined by three possible global mean sea level histories: two derived from benthic oxygen isotope records (Fig. 2, ICE-5G and WO2-derived; Peltier and Fairbanks, 2006; Waelbroeck et al., 2002) and one based on a GIA-analysis of sea-level markers (Fig. 2c, ICE-PC; Pico et al., 2017). Farmer et al. showed that, of these three options, only the relative sea level prediction with the highest peak global mean sea level prior to the LGM (−38 m) is consistent with the timing of Bering Strait flooding prior to ~36 ka, documented in the foraminifera-bound nitrogen isotope record in the Arctic (Fig. 2; Farmer et al., 2023). A peak global mean sea level near −40 m in the 15–30 kyr prior to the LGM is consistent with recent work suggesting that the Laurentide Ice Sheet grew rapidly in the time period preceding the LGM (Dalton et al., 2019, 2022; Pico et al., 2017, 2018). Whether the Laurentide Ice Sheet grew slowly or suddenly is a subject of active debate (Miller and Andrews, 2019), with important implications for our understanding of couplings between climate forcings and ice volumes across glacial cycles (Niu et al., 2024).

The deglacial timing of Bering Strait flooding since the LGM has been dated to ~11.5 ka, based on marine sediment core material that records either subaerial or marine environments, or marine transgressions (Elias et al., 1996; Hill and Driscoll, 2008; Jakobsson et al., 2017; Keigwin et al., 2006). Nevertheless, the appearance of species endemic to the Pacific in the Arctic dates a Pacific-Arctic connection (Bering Strait flooding) to nearly two thousand years earlier at ~13.3 ka (Dyke et al., 1996; Dyke and Savelle, 2001; England and Furze, 2008). Although these records disagree on the timing of flooding, recent work reconciled these records by showing that nearby ice sheet variations can lead to a sea level standstill at the Bering Strait across these time intervals. This analysis highlights the first-order control of nearby ice sheet growth and melt, especially rapid collapse events, on Bering Strait relative sea level (Pico et al., 2020).

5. Paleogenomics

5.1. Background

In certain environments, like the cold permafrost landscape of Beringia, DNA can remain preserved in physical remains for thousands of years. Ancient DNA (aDNA) has been recovered from hair, teeth, mummified tissues, bones, and even sediment, offering insights into individual and community genetics of the deep past (Fig. 5; Orlando et al., 2021).

There are two types of aDNA that are recovered from ancient animal specimens (Fig. 5): mitochondrial (mtDNA) and nuclear (nDNA). DNA originating from mitochondria is strictly matrilineal, passed from parent to offspring via the egg (Merheb et al., 2019). Each cell can contain hundreds or thousands of mitochondria depending on its function, which increases the likelihood of recovering a comprehensive mitochondrial genome from an ancient sample (Fig. 5). The abundance and matrilineal characteristic of mtDNA makes it valuable for population geneticists studying long-term species dynamics (Hundertmark et al., 2002; Llamas et al., 2016; Merheb et al., 2019). In contrast, there tend to be many fewer copies of the nuclear genome per cell, reducing the likelihood of recovering a useable nuclear genome from a degraded sample. However, the nuclear genome is much larger and contains more information than the mitochondrial genome (Rizzi et al., 2012). Nuclear DNA datasets can achieve a finer spatial and temporal resolution than mtDNA when studying local population dynamics, such as population size change or the random genetic drift of an isolated population, and are useful in deciphering intraspecific phylogenies.

Phylogenetics of ancient individuals, using either mitochondrial or nuclear genomes, in tandem with molecular clock estimation and radiocarbon dating is a useful technique for estimating the timing of population divergence and migration. In the context of the BLB, the most direct strategy involves observing the occurrence of individuals with

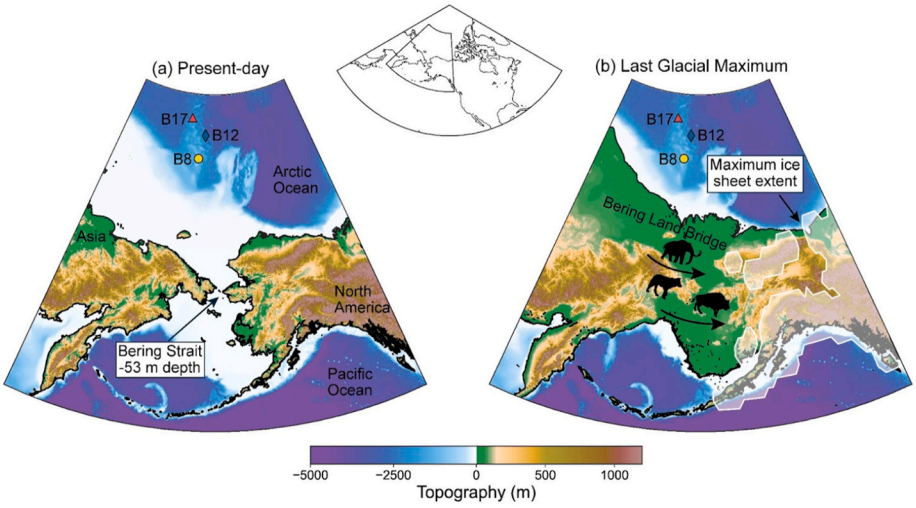

Fig. 1. a) Topography of Beringia at present-day. b) Topography of Beringia at the Last Glacial Maximum (26 ka; GMSL = −130) corrected for glacial isostatic adjustment based on the ICE-PC deglacial ice history (Pico et al., 2017). Red triangle, blue diamond, and yellow circle correspond to core sites B17, B12, and B8, respectively. White shading in panel b represents Last Glacial Maximum ice sheet extent.

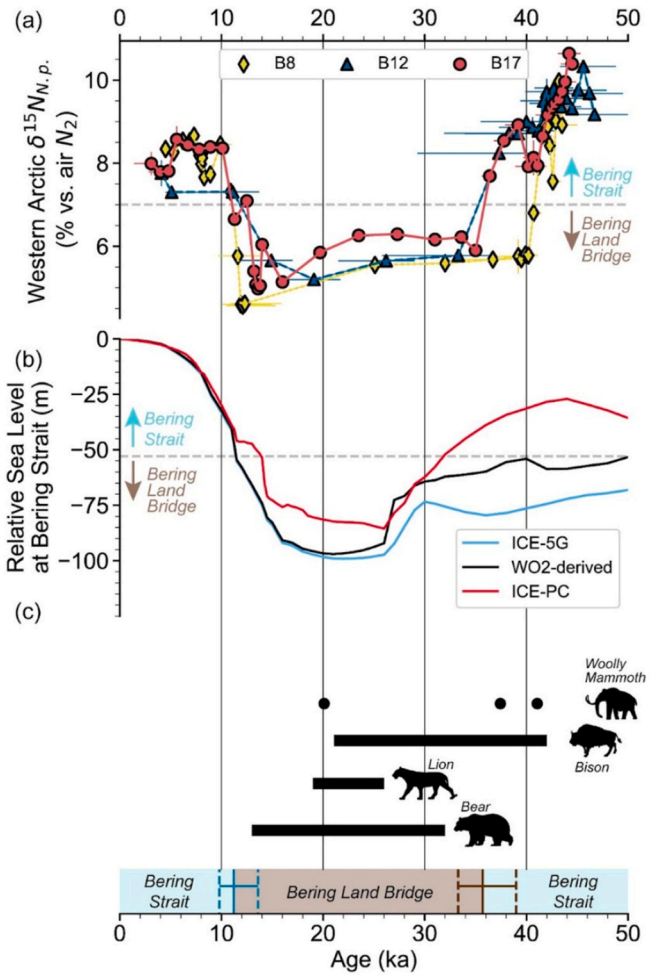

Fig. 2. a) Western Arctic foraminifera-bound nitrogen isotopes (expressed as $\delta^{15}N$) for core sites B17 (red), B12 (blue), and B8 (yellow; Farmer et al., 2023). Horizontal error bars represent 95 % confidence intervals of the age-depth model for each core. Vertical error bars represent the larger error of either measured or long-term replicate $\delta^{15}N$ precision. Horizontal dashed line at 7 ‰ represents a value above which the Bering Strait is interpreted to be open (Farmer et al., 2023). **b)** Relative sea level at the Bering Strait predicted with ice histories ICE-5G (global mean sea level based on oxygen isotope record pre-Last Glacial Maximum; blue; Argus and Peltier, 2010), ICE-PC (global mean sea level based on GIA-analysis of sea-level markers; red; Pico et al., 2017), and WO2-derived (global mean sea level based on a benthic oxygen isotope record; black; Waelbroeck et al., 2002). Gray dashed line denotes the modern sill depth of the Bering Strait (−53 m). **c)** Times of land migration across the Bering Land Bridge into North America recorded by paleo-genomic and paleontological records of woolly mammoths (Chang et al., 2017), bison (Froese et al., 2017), lions (Salis et al., 2021), and bears (Anijalg et al., 2018). Solid bars indicate molecular clock estimates of migration timing. Dots indicate the radiocarbon dates of Siberian-haplotype remains unearthed in North America. Blue bars indicate periods of Bering Strait flooding, with a blue vertical line marking the time of postglacial Bering Strait flooding and dashed lines representing a 95 % confidence interval (Farmer et al., 2025; Jakobsson et al., 2017; Pico et al., 2020). Brown bar represents BLB exposure, with a brown vertical line marking the timing of Bering Land bridge formation recorded by Western Arctic foraminifera-bound nitrogen isotopes in panel a and dashed lines marking a 95 % confidence interval (Farmer et al., 2023).

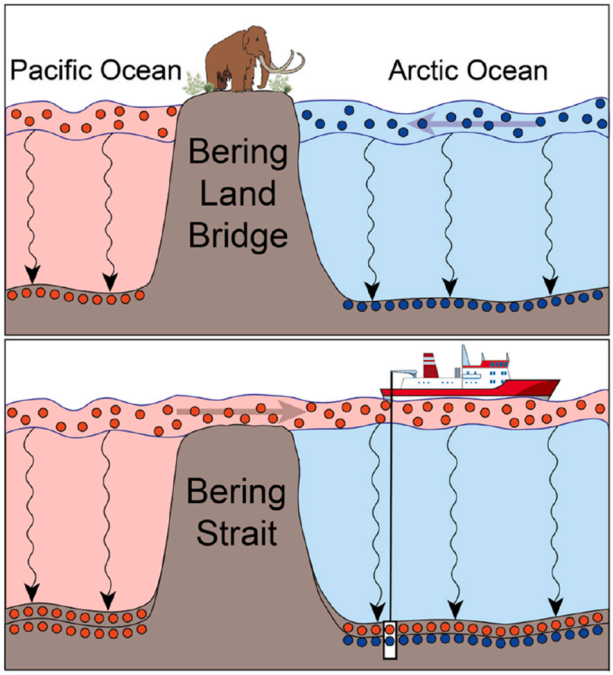

Fig. 3. Schematic illustration of how Pacific water inflow is recorded in Arctic Ocean sediments. Red (blue) shading and filled circles indicate Pacific-sourced (Atlantic-sourced) waters and sedimentary materials deriving from those waters, respectively. During intervals of low sea level (top), exposure of the Bering Land Bridge restricted Pacific water inflow to the Arctic Ocean and Arctic sedimentation was characterized by materials deriving from the Atlantic (blue circles). During intervals of high sea level (bottom), flooding of the Bering Strait allowed for inflow of less dense Pacific waters, and sediments reaching the Arctic seafloor carried a Pacific signature (red circles). Sediment cores collected via icebreakers today (bottom right) allow for reconstruction of past changes between a flooded Bering Strait and an exposed BLB based on the origin of sediment.

Siberian haplotypes in East Beringia, and vice versa, by sequencing DNA from ancient sources such as, most commonly, bone. Reliable dating techniques are necessary to translate this genetic information into estimates of migration timing. For specimens that are younger than 50 ka, radiocarbon dating is the most often used technique (Bronk Ramsey, 2008). However, to be useful for estimating migration timing, this method requires the preservation of physical remains of the migrant individuals from the time period of interest. Molecular clock dating can constrain timing even in the absence of directly dated fossils by using known or inferred DNA mutation rates to estimate the evolutionary divergence time between two or more individuals (Ho and Duchêne, 2014). Within living cells, imperfect DNA replication machinery introduces random mutations over time (Bromham, 2011). If the rate at which these mutations are introduced is known, it can be used to estimate the time required for those multiple genomes to arise from a common ancestor, also known as divergence time (dos Reis et al., 2016). Estimates of divergence for clades which appear to have cross the BLB can inform when initial migration events may have occurred, even in the absence of fossils dating to the inferred divergence time. Since mutation rates are not always constant through time, across the genome, or between species, a Bayesian method is often used to compensate for this potential uncertainty (dos Reis et al., 2016).

While sea level analyses and marine sediment isotopic data provide evidence of the exposure of the BLB, aDNA studies offer a complementary view into the role of the BLB as a conduit of gene flow between North America and Eurasia. A flooded Bering Strait prevents migration of species between the continents, causing genetic isolation between populations, whereas an exposed land bridge allows for movement, and therefore gene flow between previously isolated populations. Traces of this interbreeding between populations, or admixture, exist in the genomes of ancient animals within mitochondrial haplogroups and nDNA. Since gene flow between eastern and western populations could only occur when these populations were connected, we posit that periods of

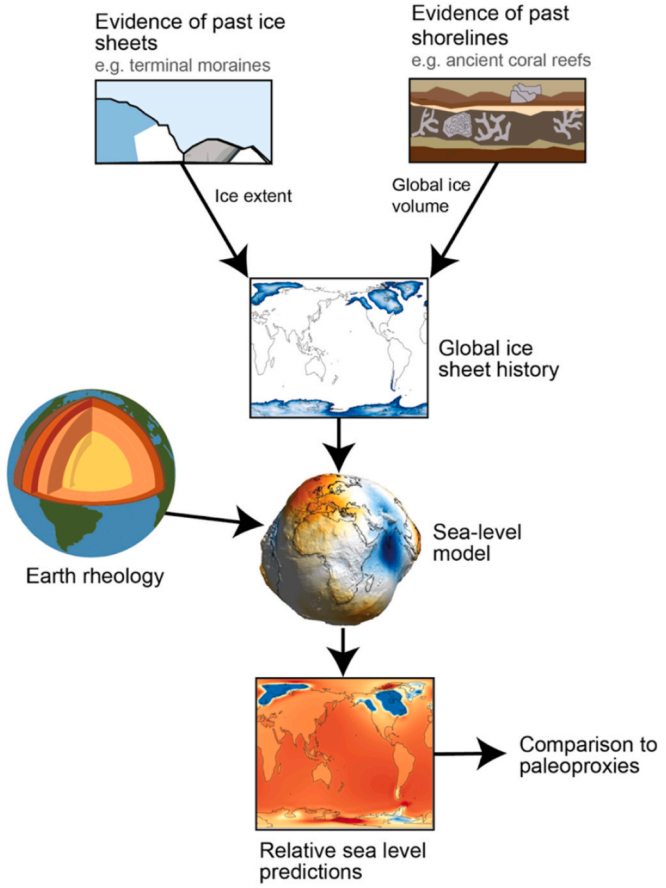

Fig. 4. Schematic describing the workflow for predicting paleo-sea-level. First, ice sheet extent and global ice volume are estimated from paleoproxies such as terminal moraines and ancient coral reefs and are used to reconstruct global ice sheet history. The global ice history is paired with a model of Earth's rheology to model gravitational and solid-Earth response to changes in ice loading (i.e., glacial isostatic adjustment). Predictions of relative sea level are compared with paleoproxies (e.g., foraminifera-bound N isotopes; Fig. 3; Farmer et al., 2023).

admixture correspond to BLB exposure.

5.2. Genetic evidence for trans-Beringian migration

5.2.1. Bison

Bison are an ideal model system for examining population dynamics across Beringia, as they are abundant in the fossil record and maintained a continual presence in Beringia throughout the last ice age, surviving the megafaunal extinctions that occurred around the LGM (Guthrie, 1989). This prevalence and continuity of the fossil record allow for tracking population dynamics through time. Dense sampling of bison mitochondrial genomes revealed that all North American bison maternal lineages most recently share an ancestor approximately 150,000 years ago, indicating when bison first arrived in North America (Froese et al., 2017). The two oldest North American bison fossils, dating to 130 and 120 ka, have very similar mitochondrial haplotypes, suggesting a single wave of migration and population expansion. Following closure of the BLB after this initial expansion, bison on either side of Beringia began genetically differentiating, and secondary contact between these divergent groups can be used to refine the timing of re-emergence of the BLB. The major evidence for such secondary contact is the appearance of Siberian-like mitochondrial haplotypes in North America, which first appear in bison dated to ~15 ka. A molecular clock dating approach indicates that the common ancestor of these bison is estimated to be sometime immediately before or during the LGM (Fig. 2c; Froese et al., 2017). Based on a reduced dataset of mitochondrial genomes that only included genetic regions that could be confidently determined in the oldest bison specimen, Froese et al. determined a conservative range of ~45-21 ka. Using the complete dataset of full bison mitochondrial genomes, this range narrows to ~36–22 ka (Froese et al., 2017). Uncertainty in point estimates of the divergences, and 9 kyr discrepancy between these estimates made between the two datasets, is due to uncertainties inherent to molecular clock calculations. Both estimates suggest movement from Siberia into North America shortly before the LGM, though since East Beringia has been more densely sampled with aDNA, it is possible that movement from East Beringia into West Beringia also occurred (Froese et al., 2017).

5.2.2. Mammoths

Unlike bison, mammoths have a much deeper history on both sides of BLB, with a presence in North America dating back over a million years (Lister and Sher, 2015). Two main mitochondrial clades appear in Beringian mammoths, 1C in North America and 1DE in Siberia (Chang et al., 2017; Enk et al., 2016). As is the case with bison, Siberian 1DE haplotypes appear in North America, starting with mammoths that have been radiocarbon dated to ~41 ka (Fig. 2c), suggesting movement from West to East Beringia around this time (Chang et al., 2017; Enk et al., 2016). As North American 1C haplotypes do not appear in Siberia at this time, this movement is assumed to be unidirectional. Before 41 ka, East Beringian mammoths fell within the North American clade, indicating that passage between the continents previously was not available.

5.2.3. Bears and lions

Though carnivores, including bears and lions, are found much more sparsely across the Beringian landscape than herbivores, they nonetheless offer additional sources of information for using population dynamics to understand movement across the BLB over the last 50 kyr. Molecular clock analysis of clade 3a1 brown bear (*Ursus arctos*) mitochondrial genomes indicate that while East and West Beringian populations diverged ~34 ka, the most recent common ancestor of clade 3a1 Alaskan brown bears lived between 32 and 13 ka (Fig. 2c; Anijalg et al., 2018), indicating that the Alaskan population spent some time in genetic isolation before entering North America, likely either on or west of the BLB. Before this time, East Beringian brown bears belonged to clade 3c and, based on molecular clock estimates, entered North America sometime between ~75 and 62 ka (Salis et al., 2021). Between 35 and 22 ka, brown bears are absent from the East Beringian fossil record, suggesting a local extinction, perhaps due to competition with giant short-faced bears (Salis et al., 2021).

Cave lions (*Panthera spelaea*) display a remarkably similar pattern of multiple movements from West to East Beringia during the Late Pleistocene, based on the coalescence of the *P. spelaea* clade 2 haplotypes from East Beringian individuals (Salis et al., 2021). Two lineages of North American clade 2 lions diverged from Eurasian lions ~33 ka (Salis et al., 2021). The timings of the most recent common ancestor of both of these North American subclades are similar to one another, with one dating to 24–22 ka the other dating to 26–19 ka (Fig. 2c; Salis et al., 2021). This pattern again suggests that the population was isolated for ~10 ka after splitting from the Eurasian population and before moving into North America. Like brown bears, cave lions reappear in the East Beringian fossil record around 22 ka after a hiatus of ~10 ka (Salis et al., 2021). Lions present pre-LGM are estimated to have entered North America between ~67 and 59 ka, according to molecular clock analyses (Salis et al., 2021).

6. Discussion

Recent datasets, developed separately, highlight new understandings of the timing of the exposure and eventual flooding of the BLB during the last 50 kyr. Evidence from paleoceanography, sea level reconstructions, and paleogenomics indicates that the BLB was last exposed soon before

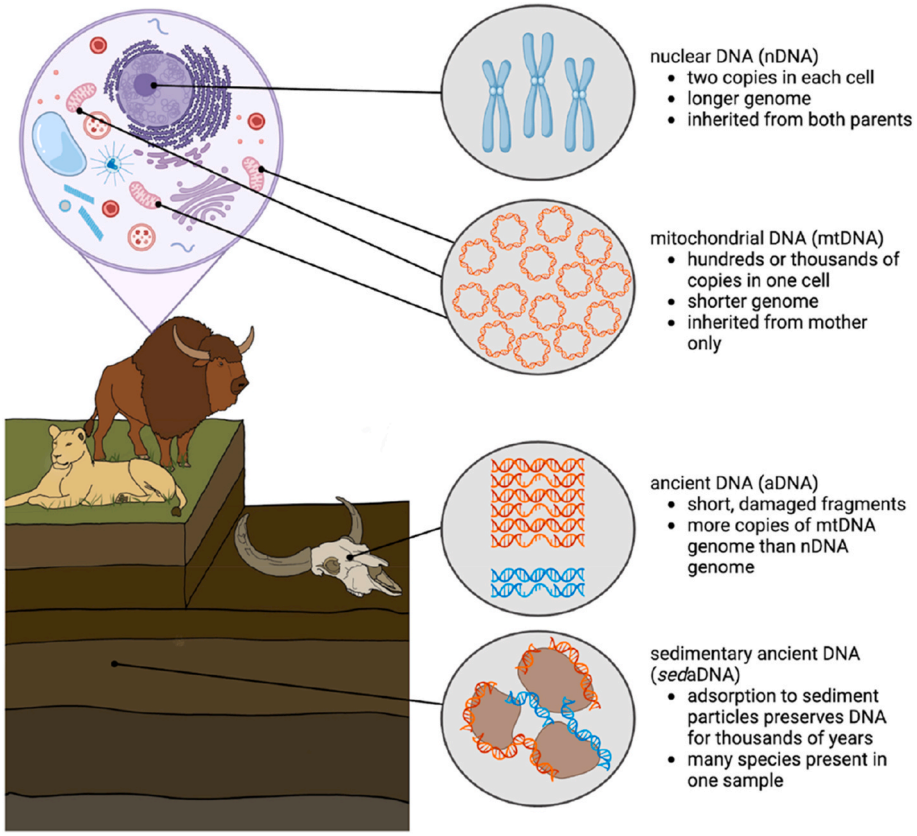

Fig. 5. Sources of nuclear, mitochondrial, ancient, and sedimentary ancient DNA. Nuclear and mitochondrial DNA are both found in the cell, although in different places and quantities. Each cell contains two copies of the nuclear genome, one copy from each parent, organized into chromosomes. Different cell types contain 100 to 10,000 copies per cell of the mitochondrial genome (Rizzi et al., 2012), which is organized into a single circular chromosome and is inherited matrilineally. Over time, both nuclear and mtDNA break down into short, damaged fragments that require specialized laboratory work to extract from ancient specimens (Dabney et al., 2013). Mitochondrial genomes are more abundant and thus more likely to be recovered compared to nuclear genomes. Nuclear genomes contain information from both maternal and paternal lineages and are more informative for certain applications. While aDNA from a single specimen is useful for reconstructing demographic history of the source species, *sed*aDNA can give insight into whole ecosystems (Giguet-Covex et al., 2019). During life and death, organisms shed DNA into their environments, where it adsorbs onto sediment particles. In ideal conditions, *sed*aDNA can be preserved for thousands or millions of years (Giguet-Covex et al., 2019; Kjær et al., 2022), allowing for ancient ecosystem reconstructions from a few grams of sediment. Created in BioRender. https://BioRender.com/n74b227.

the LGM. From a paleooceanography perspective, a geochemical proxy indicates that the last inflow of Pacific waters into the Arctic Ocean occurred ~36 ka (Fig. 2a), providing evidence for an open, but shoaling, Bering Strait at this time (Farmer et al., 2023). Genetic signatures of admixture from mammoths, bison, lions, and bears crossing the BLB generally agree with this time frame. Phylogenetic analyses of these species along with molecular clock and radiocarbon dating indicate that the BLB became passable for migration sometime between 45 and 35 ka (Fig. 2c). Recent relative sea level reconstructions for Beringia predict that the Bering Strait would be flooded to ~25 m deep between 50 and 37 ka (Fig. 2b, red line; Farmer et al., 2023; Pico, 2022).

When considered together, these datasets provide evidence for a late exposure of the BLB before the LGM, but the genetic record suggests that there may have been migration before paleoceanographic and sea level records indicate that the BLB was exposed. Estimates for bison, bear, and lion migrations are based on molecular clock dating, a method that is prone to uncertainties. The earliest radiocarbon-dated specimen is a clade 1DE mammoth from East Beringia that is dated to ~41 ka (Fig. 2c; Chang et al., 2017; Enk et al., 2016), which is 4 kyr earlier than nitrogen isotopes suggest the cessation of transport across the Bering Strait due to BLB exposure (Farmer et al., 2023). This seemingly early arrival may result from uncertainties in one or multiple proxies. For example, the timing of BLB exposure based on sea-level reconstructions is an outcome of interpolating global mean sea level between a peak at 44 ka and the LGM lowstand at 26 ka. The timing of peak global mean sea level is uncertain, likely between 50 and 35 ka (Pico et al., 2017). Last, there exists uncertainty in the absolute dating of BLB exposure from the marine records given limited knowledge of past marine reservoir ages and inter-core spread in the reconstructed timing of BLB exposure (Fig. 2a).

Notwithstanding uncertainty on exact ages, the broad concordance of terrestrial, marine, and sea level predictions of BLB exposure between 40 and 35 ka has implications for the history of human migration into the Americas. Although a land bridge may not have been strictly necessary for humans to enter North America via Siberia (Kunz and Mills, 2021; Raghavan et al., 2014), genetic and archeological evidence suggests that humans did inhabit Beringia immediately before and during the LGM (Hoffecker et al., 2023; Llamas et al., 2016; Raghavan et al., 2015). The Beringian Standstill Hypothesis, for example, suggests based on mtDNA evidence that humans migrating from Siberia into North America must have paused somewhere in Beringia for thousands of years during the LGM before continuing to populate the rest of the Americas (Tamm et al., 2007). Thus, the timing of BLB exposure has implications for the habitats and resources available to the early inhabitants of this region. Current evidence suggests that the full glacial climate of the BLB was relatively mild and mesic (Elias and Crocker, 2008) but further work to reconstruct the biota of the BLB is needed to understand if it would have been hospitable to long-term human habitation during the LGM.

7. Future directions

7.1. Paleoceanography

Although paleoceanographic reconstructions of past Bering Strait inflow to the Arctic Ocean are in their (relative) infancy, two future directions appear promising. The first involves better understanding how the "fingerprints" of Pacific-sourced waters in the Arctic Ocean are generated. Today, these fingerprints arise from strong biogeochemical cycling on the shallow, highly productive Bering and Chukchi Shelves (e.g., Whitmore et al., 2025). Understanding how these cycles are modified by variations in the extent and depth of Arctic shelves under past sea levels would allow for moving from qualitative reconstructions of Bering Strait presence/absence to quantitative reconstructions of past Bering Strait transport.

Second, the chronological frameworks for Arctic Ocean sediment records must be improved. The major advantage of sediment core-based reconstructions of past Bering Strait inflow lies in their continuity. However, telling time in Arctic Ocean sediments remains a significant challenge, even within intervals where radiocarbon dating may be applied (e.g., Hillaire-Marcel et al., 2022; Polyak et al., 2009; Razmjooei et al., 2023; Wollenburg et al., 2023). An advantage to the interdisciplinary approach used here is that the coherent insights on BLB history from terrestrial migrations and marine cores (Fig. 2) validates the existing sedimentary age model constructions for the Arctic Ocean. Future chronological refinements could be realized through continued integration of marine records with well-dated terrestrial records in Beringia, for example through the use of cryptotephras to anchor marine chronologies (e.g., Pearce et al., 2017; Reyes et al., 2022).

7.2. Sea level reconstructions

Improved chronology of Bering Strait flooding histories can better constrain both North American ice sheet geometries and in addition to global sea level variations. In particular, Bering Strait relative sea level is strongly influenced by sea-level changes linked to the loss or gain of gravitational pull from melting or growing ice sheets, in addition to the longer-term crustal deformation associated with the viscoelastic relaxation of the mantle in response to ice and ocean water loading variations (Pico et al., 2020). Conversely, improved constraints on North American ice sheet histories, especially of the nearby Cordilleran Ice Sheet whose history over the last glaciation phase is highly unconstrained (Seguinot et al., 2016), will improve our accuracy in predicting when the Bering Strait was flooded or exposed. New and improved relative sea level records around Beringia, either from submerged regions of the shelf or along the Northwestern Alaskan shoreline, will fill gaps in our understanding of regional sea level in addition to providing constraints on ice sheet history and earth structure via glacial isostatic adjustment modeling, especially if any of these records date to pre-LGM.

Additionally, relative sea level at the Bering Strait likely influences Beringian climate, as continental shelf exposure can impact local moisture transportation and precipitation (Bartlein et al., 2015; Daniels et al., 2021; Patterson et al., 2023). Therefore, quantifying the impact of Bering Strait exposure on Beringian climate, paired with an improved record of Bering Strait exposure and flooding will provide additional context for Beringian paleoclimate records (Guo et al., 2025).

7.3. Paleogenomics

Although the literature on gene flow across the BLB is rich, there are relatively few studies that have attempted to use genetic information to constrain the timing of a passable land bridge before the LGM. Reanalyzing existing datasets to look for genetic signatures of gene flow between 40 and 30 ka in a greater range of species would be a useful addition to the existing evidence already described here. For example, examining the Late Pleistocene migration history of marine mammals would provide valuable insight into the navigability of the Bering Strait, and thus further constrain the timing of BLB exposure and inform studies on ancient sea level reconstructions. Genomic data for some marine mammals such as gray whales (Alter et al., 2007) exist, but have not been evaluated in the context of Bering Strait migrations. In addition, a re-analysis of existing mammoth data to investigate this question more explicitly is necessary to strengthen evidence of migration for this species.

More work is necessary to refine the timing of horse migration during the last 50 ka. Horses dispersed across the BLB in at least two major dispersal events, one between 950 and 450 ka and another between 200 and 50 ka (Vershinina et al., 2021). These dispersals coincide with glacial cycles during which the BLB likely saw intervals of flooding and exposure. Vershinina et al. (2021) found evidence for bidirectional gene flow between North American and Eurasian horse populations in both nuclear and mitochondrial datasets, suggesting that the horses used the BLB whenever it was passable. Running Horse Collin et al. (2025) found evidence for admixture sometime before 20 ka, but some admixed specimens beyond the limit of radiocarbon make the exact timing in relation to the exposure of the BLB unclear (Running Horse Collin et al., 2025).

Improved methods for extracting and analyzing sedimentary ancient DNA (*sed*aDNA) are valuable for paleoecological reconstructions at the ecosystem level. Unlike DNA extracted from physical remains, which can only provide information about one species, *sed*aDNA represents the plants and animals present on the landscape concurrently (Fig. 5). Existing *sed*aDNA studies in Beringia have revealed ecosystem shifts with climate warming at the Pleistocene-Holocene transition (Murchie et al., 2021). Recent studies have isolated phylogenetic information from *sed*aDNA, unlocking a new tool for understanding population ancestry when fossils are scarce (Murchie et al., 2022; Pedersen et al., 2021). Given robust core chronologies, studies could be conducted to assess vegetation changes when the BLB is flooded versus exposed and to track the arrival of Siberian haplotypes in North America to provide more insight into the timing and direction of admixture across the BLB. Combined with other proxies, *sed*aDNA studies can bolster evidence for the timing of BLB exposure and flooding.

8. Conclusion

As the only point of terrestrial connection between Eurasia and the Americas, the BLB was an important corridor for biotic interchange and evolution. When flooded, the Bering Strait is a similarly important conduit between the Pacific and Arctic Oceans, with ramifications for local and global climate. Here, we combine interdisciplinary datasets to provide further evidence that the BLB was last exposed shortly before the LGM, later than previous estimates (Hu et al., 2012). Although each dataset includes some level of uncertainty, together they provide increasingly robust evidence for a later exposure and emphasize the importance of interdisciplinary approaches to studying complex paleoecological problems. In the broad disciplines of paleoecology and paleoclimate, cross-disciplinary datasets can reveal connections between fields that previously worked in isolation from one another. Data from disparate fields can cross-validate findings and provide insight into problems that cannot be solved by one dataset alone. Our results highlight the importance of interdisciplinary collaboration when studying the ancient past.

CRediT authorship contribution statement

Ciara Wanket: Writing – review & editing, Writing – original draft, Visualization, Conceptualization. **Samuel Kodama:** Writing – review & editing, Writing – original draft, Visualization, Conceptualization. **Jonas Oppenheimer:** Writing – original draft, Conceptualization. **Scott Cocker:** Writing – review & editing, Conceptualization. **Emma Steigerwald:** Conceptualization, Visualization, Writing – review & editing.

Duane Froese: Writing – review & editing, Conceptualization. **Beth Shapiro:** Writing – review & editing, Conceptualization. **Tamara Pico:** Writing – review & editing, Visualization, Conceptualization. **Jesse Farmer:** Writing – review & editing, Writing – original draft, Visualization, Conceptualization.

Declaration of competing interest

The authors declare that they have no known competing financial interests or personal relationships that could have appeared to influence the work reported in this paper.

Acknowledgements

CW recognizes support from the National Science Foundation under Award Number 2131589 and the National Institute of Health under Fellowship T32HG012344 during the writing of this manuscript. TP recognizes support from the National Science Foundation under Award OCE-2054757. JF was supported by the National Science Foundation under Award OCE-2327031. ES was supported by the Presidential Postdoctoral Fellowship Program and the National Science Foundation Postdoctoral Research Fellowship Program.

Data availability

Datasets synthesized for this review are indicated in the manuscript file.

References

Aagaard, K., Carmack, E.C., 1989. The role of sea ice and other fresh water in the arctic circulation. J. Geophys. Res.: Oceans 94 (C10), 14485–14498.

Abyzova, G.A., Neretina, T.V., Nikitin, M.A., Shapkina, A.O., Vereshchaka, A.L., 2025. Marine highways and barriers: a case study of limacina helicina phylogeography across the Siberian arctic shelf seas. Diversity 17 (8). https://doi.org/10.3390/d17080522. Article 8.

Ager, T.A., Phillips, R.L., 2008. Pollen evidence for late Pleistocene bering land bridge environments from Norton Sound, northeastern Bering Sea, Alaska. Arctic Antarct. Alpine Res. 40 (3), 451–461. https://doi.org/10.1657/1523-0430(07-076 [AGER]2.0.CO;2.

Alkire, M.B., Rember, R., Polyakov, I., 2019. Discrepancy in the identification of the atlantic/pacific front in the central Arctic Ocean: NO versus nutrient relationships. Geophys. Res. Lett. 46 (7), 3843–3852.

Alter, S.E., Rynes, E., Palumbi, S.R., 2007. DNA evidence for historic population size and past ecosystem impacts of gray whales. Proc. Natl. Acad. Sci. 104 (38), 15162–15167. https://doi.org/10.1073/pnas.0706056104.

Anijalg, P., Ho, S.Y.W., Davison, J., Keis, M., Tammeleht, E., Bobowik, K., Tumanov, I.L., Saveljev, A.P., Lyapunova, E.A., Vorobiev, A.A., Markov, N.I., Kryukov, A.P., Kojola, I., Swenson, J.E., Hagen, S.B., Eiken, H.G., Paule, L., Saarma, U., 2018. Large-scale migrations of brown bears in eurasia and to North America during the late Pleistocene. J. Biogeogr. 45 (2), 394–405. https://doi.org/10.1111/jbi.13126.

Argus, D.F., Peltier, W.R., 2010. Constraining models of postglacial rebound using space geodesy: a detailed assessment of model ICE-5G (VM2) and its relatives. Geophys. J. Int. 181 (2), 697–723. https://doi.org/10.1111/j.1365-246X.2010.04562.x.

Austermann, J., Mitrovica, J.X., Latychev, K., Milne, G.A., 2013. Barbados-based estimate of ice volume at last glacial maximum affected by subducted plate. Nat. Geosci. 6, 553–557. https://doi.org/10.1038/ngeo1859.

Bartlein, P.J., Edwards, M.E., Hostetler, S.W., Shafer, S.L., Anderson, P.M., Brubaker, L. B., Lozhkin, A.V., 2015. Early-holocene warming in beringia and its mediation by sea-level and vegetation changes. Clim. Past 11 (9), 1197–1222. https://doi.org/10.5194/cp-11-1197-2015.

Batchelor, C.L., Margold, M., Krapp, M., Murton, D.K., Dalton, A.S., Gibbard, P.L., Stokes, C.R., Murton, J.B., Manica, A., 2019. The configuration of northern hemisphere ice sheets through the Quaternary. Nat. Commun. 10, 3713. https://doi.org/10.1038/s41467-019-11601-2.

Berends, C.J., de Boer, B., van de Wal, R.S.W., 2021. Reconstructing the evolution of ice sheets, sea level, and atmospheric CO_2 during the past 3.6 million years. Clim. Past 17 (1), 361–377. https://doi.org/10.5194/cp-17-361-2021.

Bluhm, B.A., Kosobokova, K.N., Carmack, E.C., 2015. A tale of two basins: an integrated physical and biological perspective of the deep Arctic Ocean. Prog. Oceanogr. 139, 89–121.

Brierley, C.M., Fedorov, A.V., 2016. Comparing the impacts of Miocene–Pliocene changes in inter-ocean gateways on climate: Central American seaway, bering strait, and Indonesia. Earth Planet Sci. Lett. 444, 116–130. https://doi.org/10.1016/j.epsl.2016.03.010.

Bromham, L., 2011. The genome as a life-history character: why rate of molecular evolution varies between mammal species. Phil. Trans. Roy. Soc. Lond. B Biol. Sci. 366 (1577), 2503–2513. https://doi.org/10.1098/rstb.2011.0014.

Bronk Ramsey, C., 2008. Radiocarbon dating: revolutions in understanding. Archaeometry 50 (2), 249–275. https://doi.org/10.1111/j.1475-4754.2008.00394.x.

Chang, D., Knapp, M., Enk, J., Lippold, S., Kircher, M., Lister, A., MacPhee, R.D.E., Widga, C., Czechowski, P., Sommer, R., Hodges, E., Stümpel, N., Barnes, I., Dalén, L., Derevianko, A., Germonpré, M., Hillebrand-Voiculescu, A., Constantin, S., Kuznetsova, T., et al., 2017. The evolutionary and phylogeographic history of woolly mammoths: a comprehensive mitogenomic analysis. Sci. Rep. 7 (1), 44585. https://doi.org/10.1038/srep44585.

Clark, P.U., Dyke, A.S., Shakun, J.D., Carlson, A.E., Clark, J., Wohlfarth, B., Mitrovica, J. X., Hostetler, S.W., McCabe, A.M., 2009. The last glacial maximum. Science 325 (5941), 710–714. https://doi.org/10.1126/science.1172873.

Coachman, L.K., Aagaard, K., 1966. On the water exchange through bering strait. Limnol. Oceanogr. 11 (1), 44–59.

Dabney, J., Meyer, M., Pääbo, S., 2013. Ancient DNA damage. Cold Spring Harbor Perspect. Biol. 5 (7), a012567. https://doi.org/10.1101/cshperspect.a012567.

Dalton, A.S., Finkelstein, S.A., Forman, S.L., Barnett, P.J., Pico, T., Mitrovica, J.X., 2019. Was the laurentide ice sheet significantly reduced during marine isotope stage 3? Geology 47 (2), 111–114. https://doi.org/10.1130/G45335.1.

Dalton, A.S., Pico, T., Gowan, E.J., Clague, J.J., Forman, S.L., McMartin, I., Sarala, P., Helmens, K.F., 2022. The marine δ18O record overestimates Continental ice volume during marine isotope stage 3. Global Planet. Change 212, 103814. https://doi.org/10.1016/j.gloplacha.2022.103814.

Daniels, W.C., Russell, J.M., Morrill, C., Longo, W.M., Giblin, A.E., Holland-Stergar, P., Welker, J.M., Wen, X., Hu, A., Huang, Y., 2021. Lacustrine leaf wax hydrogen isotopes indicate strong regional climate feedbacks in beringia since the last ice age. Quat. Sci. Rev. 269, 107130. https://doi.org/10.1016/j.quascirev.2021.107130.

Danielson, S.L., Dobbins, E.L., Jakobsson, M., Johnson, M.A., Weingartner, T.J., Williams, W.J., Zarayskaya, Y., 2015. Sounding the Northern Seas. Eos. http://eos.org/science-updates/sounding-northern-seas.

De Boer, A.M., Nof, D., 2004. The bering Strait's grip on the northern hemisphere climate. Deep Sea Res. Oceanogr. Res. Pap. 51 (10), 1347–1366. https://doi.org/10.1016/j.dsr.2004.05.003.

de Gelder, G., Husson, L., Pastier, A.-M., Fernández-Blanco, D., Pico, T., Chauveau, D., Authemayou, C., Pedoja, K., 2022. High interstadial sea levels over the past 420ka from the huon peninsula, Papua New Guinea. Commun. Earth Environ. 3 (1), 1–12. https://doi.org/10.1038/s43247-022-00583-7.

dos Reis, M., Donoghue, P.C.J., Yang, Z., 2016. Bayesian molecular clock dating of species divergences in the genomics era. Nat. Rev. Genet. 17 (2), 71–80. https://doi.org/10.1038/nrg.2015.8.

Dyke, A., Dale, J., McNeely, R., 1996. Marine molluscs as indicators of environmental change in glaciated North America and Greenland during the last 18 000 years. Géogr. Phys. Quaternaire 50 (2), 125–184. https://doi.org/10.7202/033087ar.

Dyke, A.S., Savelle, J.M., 2001. Holocene history of the Bering Sea bowhead whale (Balaena mysticetus) in its beaufort sea summer grounds off Southwestern Victoria island. Western Canadian Arctic, Quat. Res 55, 371–379. https://doi.org/10.1006/qres.2001.2228.

Elias, S.A., Crocker, B., 2008. The bering land bridge: a moisture barrier to the dispersal of steppe-tundra biota? Quat. Sci. Rev. 27 (27), 2473–2483. https://doi.org/10.1016/j.quascirev.2008.09.011.

Elias, S.A., Short, S.K., Nelson, C.H., Birks, H.H., 1996. Life and times of the bering land bridge. Nature 382 (6586), 6586. https://doi.org/10.1038/382060a0.

England, J.H., Furze, M.F.A., 2008. New evidence from the Western Canadian arctic archipelago for the resubmergence of bering strait. Quat. Res. 70 (1), 60–67. https://doi.org/10.1016/j.yqres.2008.03.001.

Enk, J., Devault, A., Widga, C., Saunders, J.J., Szpak, P., Southon, J., Rouillard, J.M., Shapiro, B., Golding, G.B., Zazula, G.D., Froese, D.G., Fisher, D.C., MacPhee, R.D.E., Poinar, H.N., 2016. Mammuthus population dynamics in late Pleistocene North America: divergence, phylogeography, and introgression. Front. Ecology. Evolution 4. https://doi.org/10.3389/fevo.2016.00042.

Farmer, J.R., Fehrenbacher, J.S., Horner, T.J., Kast, E.R., 2025. Tools to Trace past Productivity and Ocean Nutrients. Elsevier.

Farmer, J.R., Pico, T., Underwood, O.M., Cleveland Stout, R., Granger, J., Cronin, T.M., Fripiat, F., Martínez-García, A., Haug, G.H., Sigman, D.M., 2023. The bering strait was flooded 10,000 years before the last glacial maximum. Proc. Natl. Acad. Sci. 120 (1), e2206742119. https://doi.org/10.1073/pnas.2206742119.

Farmer, J.R., Sigman, D.M., Granger, J., Underwood, O.M., Fripiat, F., Cronin, T.M., Martínez-García, A., Haug, G.H., 2021. Arctic Ocean stratification set by sea level and freshwater inputs since the last ice age. Nat. Geosci. 14 (9), 684–689. https://doi.org/10.1038/s41561-021-00789-y.

Farrell, W.E., Clark, J.A., 1976. On postglacial sea level. Geophys. J. Roy. Astron. Soc. 46 (3), 647–667. https://doi.org/10.1111/j.1365-246X.1976.tb01252.x.

Fripiat, F., Declercq, M., Sapart, C.J., Anderson, L.G., Bruechert, V., Deman, F., Fonseca-Batista, D., Humborg, C., Roukaerts, A., Semiletov, I.P., Dehairs, F., 2018. Influence of the bordering shelves on nutrient distribution in the arctic halocline inferred from water column nitrate isotopes. Limnol. Oceanogr. 63 (5), 2154–2170. https://doi.org/10.1002/lno.10930.

Froese, D., Stiller, M., Heintzman, P.D., Reyes, A.V., Zazula, G.D., Soares, A.E.R., Meyer, M., Hall, E., Jensen, B.J.L., Arnold, L.J., MacPhee, R.D.E., Shapiro, B., 2017. Fossil and genomic evidence constrains the timing of bison arrival in North America. Proc. Natl. Acad. Sci. 114 (13), 3457–3462. https://doi.org/10.1073/pnas.1620754114.

Giguet-Covex, C., Ficetola, G.F., Walsh, K., Poulenard, J., Bajard, M., Fouinat, L., Sabatier, P., Gielly, L., Messager, E., Develle, A.L., David, F., Taberlet, P., Brisset, E., Guiter, F., Sinet, R., Arnaud, F., 2019. New insights on Lake sediment DNA from the catchment: importance of taphonomic and analytical issues on the record quality. Sci. Rep. 9 (1), 14676. https://doi.org/10.1038/s41598-019-50339-1.

Goetcheus, V.G., Birks, H.H., 2001. Full-glacial upland tundra vegetation preserved under tephra in the beringia national park, seward peninsula, Alaska. Quat. Sci. Rev. 20 (1), 135–147. https://doi.org/10.1016/s0277-3791(00)00127-x.

Gowan, E.J., Zhang, X., Khosravi, S., Rovere, A., Stocchi, P., Hughes, A.L.C., Gyllencreutz, R., Mangerud, J., Svendsen, J.I., Lohmann, G., 2021. A new global ice sheet reconstruction for the past 80 000 years. Nat. Commun. 12, 1–9. https://doi.org/10.1038/s41467-021-21469-w.

Granger, J., Sigman, D.M., Gagnon, J.G., Tremblay, J.-E., Mucci, A., 2018. On the properties of the arctic halocline and deep water masses of the Canada basin from nitrate isotope ratios. J. Gephys. Res. Oceans 123, 5443–5458.

Grant, K.M., Rohling, E.J., Ramsey, C.B., Cheng, H., Edwards, R.L., Florindo, F., Heslop, D., Marra, F., Roberts, A.P., Tamisiea, M.E., Williams, F., 2014. Sea-level variability over five glacial cycles. Nat. Commun. 5, 5076. https://doi.org/10.1038/ncomms6076.

Guo, F., Huang, Y., Vachula, R., Wang, K., O'Donnell, J., Du, X., Russell, J., Clemens, S., Yeo, D., Andreev, A., Herzschuh, U., Liu, X., Liu, Y., Su, B., Santos, E., Bobik, T., Yan, M., Sun, Y., Lu, Z., Liu, Z., 2025. Precession and ice sheet control of hydroclimate in arctic east beringia over the past 240,000 years. Research Square. https://doi.org/10.21203/rs.3.rs-4515358/v1.

Guthrie, R.D., 1989. Frozen Fauna of the Mammoth Steppe: the Story of Blue Babe. University of Chicago Press. https://press.uchicago.edu/ucp/books/book/chicago/F/bo3774765.html.

Guthrie, R.D., 2001. Origin and causes of the mammoth steppe: a story of cloud cover, woolly mammal tooth pits, buckles, and inside-out beringia. Quat. Sci. Rev. 20 (1–3), 549–574. https://doi.org/10.1016/S0277-3791(00)00099-8.

Hall, J.R., Allison, M.S., Papadopoulos, M.T., Barfod, D.N., Jones, S.M., 2023. Timing and consequences of bering strait opening: new insights from 40Ar/39Ar dating of the barmur group (tjörnes beds), northern Iceland. Paleoceanogr. Paleoclimatol. 38 (4), e2022PA004539. https://doi.org/10.1029/2022PA004539.

Hanebuth, T.J.J., Saito, Y., Tanabe, S., Vu, Q.L., Ngo, Q.T., 2006. Sea levels during late marine isotope stage 3, 145–146, pp. 119–134. https://doi.org/10.1016/j.quaint.2005.07.008.

Heintzman, P.D., Zazula, G.D., Cahill, J.A., Reyes, A.V., MacPhee, R.D.E., Shapiro, B., 2015. Genomic data from extinct north American camelops revise camel evolutionary history. Mol. Biol. Evol. 32 (9), 2433–2440. https://doi.org/10.1093/molbev/msv128.

Hibbert, F.D., Rohling, E.J., Dutton, A., Williams, F.H., Chutcharavan, P.M., Zhao, C., Tamisiea, M.E., 2016. Coral indicators of past sea-level change: a global repository of U-series dated benchmarks. Quat. Sci. Rev. 145, 1–56. https://doi.org/10.1016/j.quascirev.2016.04.019.

Hill, J.C., Driscoll, N.W., 2008. Paleodrainage on the Chukchi shelf reveals sea level history and meltwater discharge. Mar. Geol. 254, 129–151. https://doi.org/10.1016/j.margeo.2008.05.018.

Hillaire-Marcel, C., de Vernal, A., Rong, Y., Roberge, P., Song, T., 2022. Challenging radiocarbon chronostratigraphies in central Arctic Ocean sediment. Geophys. Res. Lett. 49 (21), e2022GL100446. https://doi.org/10.1029/2022GL100446.

Ho, S.Y.W., Duchêne, S., 2014. Molecular-clock methods for estimating evolutionary rates and timescales. Mol. Ecol. 23 (24), 5947–5965. https://doi.org/10.1111/mec.12953.

Hoffecker, J.F., Elias, S.A., O'Rourke, D.H., 2014. Out of beringia? Science 343 (6174), 979–980. https://doi.org/10.1126/science.1250768.

Hoffecker, J.F., Elias, S.A., Scott, G.R., O'Rourke, D.H., Hlusko, L.J., Potapova, O., Pitulko, V., Pavlova, E., Bourgeon, L., Vachula, R.S., 2023. Beringia and the peopling of the Western hemisphere. Proc. Biol. Sci. 290, 20222246. https://doi.org/10.1098/rspb.2022.2246, 1990.

Hu, A., Meehl, G.A., Han, W., Timmermann, A., Otto-Bliesner, B., Liu, Z., Washington, W. M., Large, W., Abe-Ouchi, A., Kimoto, M., Lambeck, K., Wu, B., 2012. Role of the bering strait on the hysteresis of the ocean conveyor belt circulation and glacial climate stability. Proc. Natl. Acad. Sci. 109 (17), 6417–6422. https://doi.org/10.1073/pnas.1116014109.

Hu, A., Meehl, G.A., Otto-Bliesner, B.L., Waelbroeck, C., Han, W., Loutre, M.-F., Lambeck, K., Mitrovica, J.X., Rosenbloom, N., 2010. Influence of bering strait flow and north Atlantic circulation on glacial sea-level changes. Nat. Geosci. 3 (2). https://doi.org/10.1038/ngeo729. Article 2.

Hundertmark, K.J., Shields, G.F., Udina, I.G., Bowyer, R.T., Danilkin, A.A., Schwartz, C. C., 2002. Mitochondrial phylogeography of moose (alces alces): late Pleistocene divergence and population expansion. Mol. Phylogenet. Evol. 22 (3), 375–387. https://doi.org/10.1006/mpev.2001.1058.

Jakobsson, M., Pearce, C., Cronin, T.M., Backman, J., Anderson, L.G., Barrientos, N., Björk, G., Coxall, H., Boer, A., Mayer, L.A., Mörth, C.-M., Nilsson, J., Rattray, J.E., Stranne, C., Semiletov, I., O'Regan, M., 2017. Post-glacial flooding of the bering land bridge dated to 11 cal ka BP based on new geophysical and sediment records. Clim. Past 13, 991–1005. https://doi.org/10.5194/cp-13-991-2017.

Jones, E.P., Anderson, L.G., Swift, J.H., 1998. Distribution of Atlantic and Pacific waters in the upper Arctic Ocean: implications for circulation. Geophys. Res. Lett. 25 (6), 765–768.

Kaufman, D.S., Brigham-Grette, J., 1993. Aminostratigraphic correlations and paleotemperature implications, Pliocene-Pleistocene high-sea-level deposits, northwestern Alaska. Quat. Sci. Rev. 12 (1), 21–33. https://doi.org/10.1016/0277-3791(93)90046-O.

Keigwin, L.D., Donnelly, J.P., Cook, M.S., Driscoll, N.W., Brigham-Grette, J., 2006. Rapid sea-level rise and Holocene climate in the Chukchi sea. Geology 34, 861–864. https://doi.org/10.1130/G22712.1.

Kjær, K.H., Winther Pedersen, M., De Sanctis, B., De Cahsan, B., Korneliussen, T.S., Michelsen, C.S., Sand, K.K., Jelavić, S., Ruter, A.H., Schmidt, A.M.A., Kjeldsen, K.K., Tesakov, A.S., Snowball, I., Gosse, J.C., Alsos, I.G., Wang, Y., Dockter, C., Rasmussen, M., Jørgensen, M.E., et al., 2022. A 2-million-year-old ecosystem in Greenland uncovered by environmental DNA. Nature 612 (7939), 283–291. https://doi.org/10.1038/s41586-022-05453-y.

Kunz, M.L., Mills, R.O., 2021. A precolumbian presence of Venetian glass trade beads in arctic Alaska. Am. Antiq. 86 (2), 395–412. https://doi.org/10.1017/aaq.2020.100.

Lambeck, K., Chappell, J., 2001. Sea level change through the last glacial cycle. Science 292, 679–686. https://doi.org/10.1126/science.1059549.

Lambeck, K., Rouby, H., Purcell, A., Sun, Y., Sambridge, M., 2014. Sea Level and Global Ice Volumes from the Last Glacial Maximum to the Holocene, vol 111. Proceedings of the National Academy of Sciences, pp. 15296–15303. https://doi.org/10.1073/pnas.1411762111.

Lister, A.M., Sher, A.V., 2015. Evolution and dispersal of mammoths across the northern hemisphere. Science (New York, N.Y.) 350 (6262), 805–809. https://doi.org/10.1126/science.aac5660.

Llamas, B., Fehren-Schmitz, L., Valverde, G., Soubrier, J., Mallick, S., Rohland, N., Nordenfelt, S., Valdiosera, C., Richards, S.M., Rohrlach, A., Romero, M.I.B., Espinoza, I.F., Cagigao, E.T., Jiménez, L.W., Makowski, K., Reyna, I.S.L., Lory, J.M., Torrez, J.A.B., Rivera, M.A., et al., 2016. Ancient mitochondrial DNA provides high-resolution time scale of the peopling of the americas. Sci. Adv. 2 (4), e1501385. https://doi.org/10.1126/sciadv.1501385.

Loog, L., Thalmann, O., Sinding, M.-H.S., Schuenemann, V.J., Perri, A., Germonpré, M., Bocherens, H., Witt, K.E., Samaniego Castruita, J.A., Velasco, M.S., Lundstrøm, I.K. C., Wales, N., Sonet, G., Frantz, L., Schroeder, H., Budd, J., Jimenez, E.-L., Fedorov, S., Gasparyan, B., et al., 2020. Ancient DNA suggests modern wolves trace their origin to a late Pleistocene expansion from beringia. Mol. Ecol. 29 (9), 1596–1610. https://doi.org/10.1111/mec.15329.

Malatesta, L.C., Finnegan, N.J., Huppert, K.L., Carreño, E.I., 2021. The influence of rock uplift rate on the formation and preservation of individual marine terraces during multiple sea-level stands. Geology 50, 101–105. https://doi.org/10.1130/G49245.1.

Mann, D.H., Gaglioti, B.V., 2024. The Northeast Pacific Ocean and Northwest Coast of North America within the global climate system, 29,000 to 11,700 years ago. Earth Sci. Rev. 254, 104782. https://doi.org/10.1016/j.earscirev.2024.104782.

Merheb, M., Matar, R., Hodeify, R., Siddiqui, S.S., Vazhappilly, C.G., Marton, J., Azharuddin, S., Al Zouabi, H., 2019. Mitochondrial DNA, a powerful tool to decipher ancient human civilization from domestication to music, and to uncover historical murder cases. Cells 8 (5), 433. https://doi.org/10.3390/cells8050433.

Miller, G.H., Andrews, J.T., 2019. Hudson Bay was not deglaciated during MIS-3. Quat. Sci. Rev. 225, 105944. https://doi.org/10.1016/j.quascirev.2019.105944.

Moucha, R., Forte, A.M., Mitrovica, J.X., Rowley, D.B., Quéré, S., Simmons, N.A., Grand, S.P., 2008. Dynamic topography and long-term sea-level variations: there is no such thing as a stable Continental platform. Earth Planet Sci. Lett. 271, 101–108. https://doi.org/10.1016/j.epsl.2008.03.056.

Muhs, D.R., Simmons, K.R., Schumann, R.R., Groves, L.T., Mitrovica, J.X., Laurel, D., 2012. Sea-level history during the last interglacial complex on san nicolas island, California: implications for glacial isostatic adjustment processes, paleozoogeography and tectonics. Quat. Sci. Rev. 37, 1–25. https://doi.org/10.1016/j.quascirev.2012.01.010.

Murchie, T.J., Karpinski, E., Eaton, K., Duggan, A.T., Baleka, S., Zazula, G.D., MacPhee, R.D.E., Froese, D.G., Poinar, H.N., 2022. Pleistocene mitogenomes reconstructed from the environmental DNA of permafrost sediments. Curr. Biol. https://doi.org/10.1016/j.cub.2021.12.023.

Murchie, T.J., Monteath, A.J., Mahony, M.E., Long, G.S., Cocker, S., Sadoway, T., Karpinski, E., Zazula, G., MacPhee, R.D.E., Froese, D., Poinar, H.N., 2021. Collapse of the mammoth-steppe in central Yukon as revealed by ancient environmental DNA. Nat. Commun. 12 (1). https://doi.org/10.1038/s41467-021-27439-6. Article 1.

Naidu, A.S., Creager, J.S., Mowatt, T.C., 1982. Clay mineral dispersal patterns in the north bering and Chukchi seas. Mar. Geol. 47, 1–15.

Newton, R., Schlosser, P., Mortlock, R., Swift, J., MacDonald, R., 2013. Canadian basin freshwater sources and changes: results from the 2005 Arctic Ocean section. J. Geophys. Res. Oceans 118, 2133–2154. https://doi.org/10.1002/jgrc.20101.

Niu, L., Knorr, G., Krebs-Kanzow, U., Gierz, P., Lohmann, G., 2024. Rapid laurentide ice sheet growth preceding the last glacial maximum due to summer snowfall. Nat. Geosci. 17, 440–449. https://doi.org/10.1038/s41561-024-01419-z.

Orlando, L., Allaby, R., Skoglund, P., Der Sarkissian, C., Stockhammer, P.W., Ávila-Arcos, M.C., Fu, Q., Krause, J., Willerslev, E., Stone, A.C., Warinner, C., 2021. Ancient DNA analysis. Nature Rev. Methods. Prim. 1 (1), 1. https://doi.org/10.1038/s43586-020-00011-0.

Patterson, E.W., Johnson, K.R., Griffiths, M.L., Kinsley, C.W., McGee, D., Du, X., Pico, T., Wolf, A., Ersek, V., Mortlock, R.A., Yamoah, K.A., Bùi, T.N., Trần, M.X., Đỗ-Trọng, Q., Võ, T.V., Đinh, T.H., 2023. Glacial changes in sea level modulated millennial-scale variability of Southeast Asian autumn monsoon rainfall. Proc. Natl. Acad. Sci. 120 (27), e2219489120. https://doi.org/10.1073/pnas.2219489120.

Pearce, C., Varhelyi, A., Wastegård, S., Muschitiello, F., Barrientos, N., O'Regan, M., Cronin, T.M., Gemery, L., Semiletov, I., Backman, J., Jakobsson, M., 2017. The 3.6 ka aniakchak tephra in the Arctic Ocean: a constraint on the Holocene radiocarbon reservoir age in the Chukchi sea. Clim. Past 13 (4), 303–316. https://doi.org/10.5194/cp-13-303-2017.

Pedersen, M.W., De Sanctis, B., Saremi, N.F., Sikora, M., Puckett, E.E., Gu, Z., Moon, K.L., Kapp, J.D., Vinner, L., Vardanyan, Z., Ardelean, C.F., Arroyo-Cabrales, J., Cahill, J. A., Heintzman, P.D., Zazula, G., MacPhee, R.D.E., Shapiro, B., Durbin, R.,

Willerslev, E., 2021. Environmental genomics of late Pleistocene Black bears and giant short-faced bears. Curr. Biol. 31 (12), 2728–2736.e8. https://doi.org/10.1016/j.cub.2021.04.027.
Peltier, W.R., Fairbanks, R.G., 2006. Global glacial ice volume and last glacial maximum duration from an extended Barbados sea level record. Quat. Sci. Rev. 25, 3322–3337. https://doi.org/10.1016/j.quascirev.2006.04.010.
Pico, T., 2022. Toward new and independent constraints on global mean sea-level highstands during the last glaciation (marine isotope stage 3, 5a, and 5c). Paleoceanogr. Paleoclimatol. 37 (12), e2022PA004560. https://doi.org/10.1029/2022PA004560.
Pico, T., Birch, L., Weisenberg, J., Mitrovica, J.X., 2018. Refining the laurentide ice sheet at marine isotope stage 3: a data-based approach combining glacial isostatic simulations with a dynamic ice model. Quat. Sci. Rev. 195, 171–179. https://doi.org/10.1016/j.quascirev.2018.07.023.
Pico, T., Creveling, J.R., Mitrovica, J.X., 2017. Sea-level records from the U.S. mid-Atlantic constrain laurentide ice sheet extent during marine isotope stage 3. Nat. Commun. 8, 1–6. https://doi.org/10.1038/ncomms15612.
Pico, T., Mitrovica, J.X., Ferrier, K.L., Braun, J., 2016. Global ice volume during MIS 3 inferred from a sea-level analysis of sedimentary core records in the yellow river Delta. Quat. Sci. Rev. 152, 72–79. https://doi.org/10.1016/j.quascirev.2016.09.012.
Pico, T., Mitrovica, J.X., Mix, A.C., 2020. Sea level fingerprinting of the bering strait flooding history detects the source of the younger dryas climate event. Sci. Adv. 6. https://doi.org/10.1126/sciadv.aay2935.
Polyak, L., Bischof, J., Ortiz, J.D., Darby, D.A., Channell, J.E.T., Xuan, C., Kaufman, D.S., Løvlie, R., Schneider, D.A., Eberl, D.D., Adler, R.E., Council, E.A., 2009. Late Quaternary stratigraphy and sedimentation patterns in the western Arctic Ocean. Global Planet. Change 68 (1), 5–17. https://doi.org/10.1016/j.gloplacha.2009.03.014.
Porcelli, D., Andersson, P.S., Baskaran, M., Frank, M., Björk, G., Semiletov, I., 2009. The distribution of neodymium isotopes in Arctic Ocean basins. Geochem. Cosmochim. Acta 73 (9), 2645–2659. https://doi.org/10.1016/j.gca.2008.11.046.
Praetorius, S.K., Alder, J.R., Condron, A., Mix, A.C., Walczak, M.H., Caissie, B.E., Erlandson, J.M., 2023. Ice and ocean constraints on early human migrations into North America along the Pacific coast. Proc. Natl. Acad. Sci. U. S. A 120 (7), e2208738120. https://doi.org/10.1073/pnas.2208738120.
Raghavan, M., DeGiorgio, M., Albrechtsen, A., Moltke, I., Skoglund, P., Korneliussen, T. S., Grønnow, B., Appelt, M., Gulløv, H.C., Friesen, T.M., Fitzhugh, W., Malmström, H., Rasmussen, S., Olsen, J., Melchior, L., Fuller, B.T., Fahrni, S.M., Stafford, T., Grimes, V., et al., 2014. The genetic prehistory of the new world arctic. Science (New York, N.Y.) 345 (6200), 1255832. https://doi.org/10.1126/science.1255832.
Raghavan, M., Steinrücken, M., Harris, K., Schiffels, S., Rasmussen, S., DeGiorgio, M., Albrechtsen, A., Valdiosera, C., Ávila-Arcos, M.C., Malaspinas, A.-S., Eriksson, A., Moltke, I., Metspalu, M., Homburger, J.R., Wall, J., Cornejo, O.E., Moreno-Mayar, J. V., Korneliussen, T.S., Pierre, T., et al., 2015. Genomic evidence for the Pleistocene and recent population history of Native Americans. Science 349 (6250), aab3884. https://doi.org/10.1126/science.aab3884.
Raymond-Yakoubian, J., Khokhlov, Y., Yarzutkina, A., 2014. Indigenous Knowledge and Use of Bering Strait Region Ocean Currents. National Park Service. Shared Beringian Heritage Program.
Razmjooei, M.J., Henderiks, J., Coxall, H.K., Baumann, K.-H., Vermassen, F., Jakobsson, M., Niessen, F., O'Regan, M., 2023. Revision of the Quaternary calcareous nannofossil biochronology of Arctic Ocean sediments. Quat. Sci. Rev. 321, 108382. https://doi.org/10.1016/j.quascirev.2023.108382.
Reyes, A.V., Jensen, B.J.L., Woudstra, S.H., Bolton, M.S.M., Buryak, S.D., Cook, M.S., Harvey, J., Westgate, J.A., 2022. Detrital glass in a Bering Sea sediment core yields a ca. 160 ka marine isotope stage 6 age for old Crow tephra. Geology 51 (1), 106–110. https://doi.org/10.1130/G50491.1.
Rizzi, E., Lari, M., Gigli, E., De Bellis, G., Caramelli, D., 2012. Ancient DNA studies: new perspectives on old samples. Genet. Sel. Evol. 44 (1), 21. https://doi.org/10.1186/1297-9686-44-21.
Rohling, E.J., Foster, G.L., Grant, K.M., Marino, G., Roberts, A.P., Tamisiea, M.E., Williams, F., 2014. Sea-level and deep-sea-temperature variability over the past 5.3 million years. Nature 508, 477–482. https://doi.org/10.1038/nature13230.
Running Horse Collin, Y., Bataille, C.P., Hershauer, S., Hunska Tašunke Icu, M., Nujipi, A., Justin, W., Stelkia, J., C'wyelx, Stelkia, J.A., Topkok, S.A., Leonard, B.G., Soop, B., Gonzalez, M., Luta Wiŋ, A., Wiŋ, W., Omniya, T., Dull Knife, B., Mažasu, Means, B., et al., 2025. Sustainability insights from late Pleistocene climate change and horse migration patterns. Science 388 (6748), 748–755. https://doi.org/10.1126/science.adr2355.
Salis, A.T., Bray, S.C.E., Lee, M.S.Y., Heiniger, H., Barnett, R., Burns, J.A., Doronichev, V., Fedje, D., Golovanova, L., Harington, C.R., Hockett, B., Kosintsev, P., Lai, X., Mackie, Q., Vasiliev, S., Weinstock, J., Yamaguchi, N., Meachen, J.A., Cooper, A., Mitchell, K.J., 2021. Lions and brown bears colonised North America in multiple synchronous waves of dispersal across the bering land bridge. Mol. Ecol. https://doi.org/10.1111/mec.16267.
Seguinot, J., Rogozhina, I., Stroeven, A.P., Margold, M., Kleman, J., 2016. Numerical simulations of the Cordilleran ice sheet through the last glacial cycle. Cryosphere 10 (2), 639–664. https://doi.org/10.5194/tc-10-639-2016.
Serreze, M.C., Barrett, A.P., Slater, A.G., Woodgate, R.A., Aagaard, K., Lammers, R.B., Steele, M., Moritz, R., Meredith, M., Lee, C.M., 2006. The large-scale freshwater cycle of the arctic. J. Geophys. Res.: Oceans 111 (C11). https://doi.org/10.1029/2005JC003424.
Siddall, M., Rohling, E.J., Almogi-Labin, A., Hemleben, C., Meischner, D., Schmelzer, I., Smeed, D.A., 2003. Sea-level fluctuations during the last glacial cycle. Nature 423, 853–858. https://doi.org/10.1038/nature01690.
Siddall, M., Rohling, E.J., Thompson, W.G., Waelbroeck, C., 2008. Marine isotope stage 3 sea level fluctuations: data synthesis and new outlook. Rev. Geophys. 46 (4). https://doi.org/10.1029/2007RG000226.
Siddall, M., Smeed, D.A., Hemleben, C., Rohling, E.J., Schmelzer, I., Peltier, W.R., 2004. Understanding the Red Sea response to sea level. Earth Planet Sci. Lett. 225, 421–434. https://doi.org/10.1016/j.epsl.2004.06.008.
Song, T., Hillaire-Marcel, C., de Vernal, A., Liu, Y., Wang, W., Huang, Y., 2022. A reassessment of Nd-isotopes and clay minerals as tracers of the Holocene Pacific water flux through bering strait. Mar. Geol. 443, 106698. https://doi.org/10.1016/j.margeo.2021.106698.
Spratt, R.M., Lisiecki, L.E., 2016. A late Pleistocene sea level stack. Clim. Past 12, 1079–1092. https://doi.org/10.5194/cp-12-1079-2016.
Stein, R., Fahl, K., Gierz, P., Niessen, F., Lohmann, G., 2017. Arctic Ocean sea ice cover during the penultimate glacial and the last interglacial. Nat. Commun. 8 (1), 373. https://doi.org/10.1038/s41467-017-00552-1.
Stokes, C.R., Tarasov, L., Blomdin, R., Cronin, T.M., Fisher, T.G., Gyllencreutz, R., Hättestrand, C., Heyman, J., Hindmarsh, R.C.A., Hughes, A.L.C., Jakobsson, M., Kirchner, N., Livingstone, S.J., Margold, M., Murton, J.B., Noormets, R., Peltier, W. R., Peteet, D.M., Piper, D.J.W., et al., 2015. On the reconstruction of palaeo-ice sheets: recent advances and future challenges. Quat. Sci. Rev. 125, 15–49. https://doi.org/10.1016/j.quascirev.2015.07.016.
Stone, J.O., Balco, G.A., Sugden, D.E., Caffee, M.W., Sass, L.C., Cowdery, S.G., Siddoway, C., 2003. Holocene deglaciation of marie byrd land. West Antarctica, Sci/299, 99–102. https://doi.org/10.1126/science.1077998.
Tamm, E., Kivisild, T., Reidla, M., Metspalu, M., Smith, D.G., Mulligan, C.J., Bravi, C.M., Rickards, O., Martinez-Labarga, C., Khusnutdinova, E.K., Fedorova, S.A., Golubenko, M.V., Stepanov, V.A., Gubina, M.A., Zhadanov, S.I., Ossipova, L.P., Damba, L., Voevoda, M.I., Dipierri, J.E., et al., 2007. Beringian standstill and spread of native American founders. PLoS One 2 (9), e829. https://doi.org/10.1371/journal.pone.0000829.
Torres-Valdés, S., Tsubouchi, T., Bacon, S., Naveira-Garabato, A.C., Sanders, R., McLaughlin, F.A., Petrie, B., Kattner, G., Azetsu-Scott, K., Whitledge, T.E., 2013. Export of nutrients from the Arctic Ocean. J. Geophys. Res.: Oceans 118 (4), 1625–1644. https://doi.org/10.1002/jgrc.20063.
Vershinina, A.O., Heintzman, P.D., Froese, D.G., Zazula, G., Cassatt-Johnstone, M., Dalén, L., Der Sarkissian, C., Dunn, S.G., Ermini, L., Gamba, C., Groves, P., Kapp, J. D., Mann, D.H., Seguin-Orlando, A., Southon, J., Stiller, M., Wooller, M.J., Baryshnikov, G., Gimranov, D., et al., 2021. Ancient horse genomes reveal the timing and extent of dispersals across the bering land bridge. Mol. Ecol. 30 (23), 6144–6161. https://doi.org/10.1111/mec.15977.
Waelbroeck, C., Labeyrie, L., Michel, E., Duplessy, J.C., McManus, J.F., Lambeck, K., Balbon, E., Labracherie, M., 2002. Sea-level and deep water temperature changes derived from benthic Foraminifera isotopic records. Quat. Sci. Rev. 21, 295–305. https://doi.org/10.1016/S0277-3791(01)00101-9.
Whitmore, L.M., Jensen, L., Granger, J., Xiang, Y., Kipp, L., Pasqualini, A., Newton, R., Agather, A.M., Anderson, R.F., Black, E.E., Bowman, K.L., Bourbonnais, A., Brzezinski, M.A., Bundy, R.M., Charette, M.A., Edwards, R.L., Fitzsimmons, J.N., Hansell, D.A., Lam, P.J., et al., 2025. Multi-elemental tracers in the amerasian basin reveal interlinked biogeochemical and physical processes in the Arctic Ocean upper halocline. Glob. Biogeochem. Cycles 39 (4), e2024GB008342. https://doi.org/10.1029/2024GB008342.
Whitmore, L.M., Pasqualini, A., Newton, R., Shiller, A.M., 2020. Gallium: a new tracer of Pacific water in the Arctic Ocean. J. Geophys. Res.: Oceans 125 (7), 015842, 2019.
Wollenburg, J.E., Matthiessen, J., Vogt, C., Nehrke, G., Grotheer, H., Wilhelms-Dick, D., Geibert, W., Mollenhauer, G., 2023. Omnipresent authigenic calcite distorts arctic radiocarbon chronology. Commun. Earth Environ. 4 (1), 136. https://doi.org/10.1038/s43247-023-00802-9.
Woodgate, R.A., 2018. Increases in the Pacific inflow to the arctic from 1990 to 2015, and insights into seasonal trends and driving mechanisms from year-round bering strait mooring data. Prog. Oceanogr. 160, 124–154.
Wooller, M.J., Saulnier-Talbot, É., Potter, B.A., Belmecheri, S., Bigelow, N., Choy, K., Cwynar, L.C., Davies, K., Graham, R.W., Kurek, J., Langdon, P., Medeiros, A., Rawcliffe, R., Wang, Y., Williams, J.W., 2018. A new terrestrial palaeoenvironmental record from the bering land bridge and context for human dispersal. R. Soc. Open Sci. 5 (6), 180145. https://doi.org/10.1098/rsos.180145.
Yamamoto, M., Nam, S.-I., Polyak, L., Kobayashi, D., Suzuki, K., Irino, T., Shimada, K., 2017. Holocene dynamics in the bering strait inflow to the arctic and the beaufort gyre circulation based on sedimentary records from the Chukchi sea. Clim. Past 13 (9), 1111–1127. https://doi.org/10.5194/cp-13-1111-2017.
Yokoyama, Y., Lambeck, K., Deckker, P.D., Johnston, P., Keith Fifield, L., 2000. Timing of last glacial maximum from observed sea-level minima. Nature 406, 713–716.